Surface Acoustic Wave Vibration Sensors for Measuring Aircraft Flutter

William C. Wilson, Jason P. Moore, Peter D. Juarez
Nondestructive Evaluation Sciences Branch
NASA Langley Research Center
Hampton, VA, USA
William.C.Wilson@nasa.gov

***Abstract*— Under NASA's Advanced Air Vehicles Program the Advanced Air Transport Technology (AATT) Project is investigating flutter effects on aeroelastic wings. To support that work a new method for measuring vibrations due to flutter has been developed. The method employs low power Surface Acoustic Wave (SAW) sensors. To demonstrate the ability of the SAW sensor to detect flutter vibrations the sensors were attached to a Carbon fiber–reinforced polymer (CFRP) composite panel which was vibrated at six frequencies from 1Hz to 50Hz. The SAW data was compared to accelerometer data and was found to resemble sine waves and match each other closely. The SAW module design and results from the tests are presented here.**

Keywords- SHM, IVHM, SAW, Surface Acoustic Wave, Fluttter, Sensors

I. INTRODUCTION

Under NASA's Advanced Air Vehicles Program the Advanced Air Transport Technology (AATT) Project is investigating flutter effects in aeroelastic wings. One sub portion of the program, called Subsonic Ultra-Green Aircraft Research (SUGAR), is examining the aeroelasticity of high aspect ratio wings such as the truss-braced wing design [1, 2]. It is estimated that truss braced wings could reduce aircraft fuel consumption by 5~10% when compared to today's conventional wings. NASA is also investigating the behavior of light-weight flexible aircraft structures using the X-56 Multi-Utility Technology Testbed (MUTT) [3], an unmanned aircraft system consisting of two center-bodies and four sets of interchangeable wings of varying aeroelasticity.

While flexible high aspect ratio wings may lead to more efficient aircraft, they may also lead to increased flutter conditions and onset of flutter at lower speeds of operation [4]. Therefore, flutter suppression is necessary for highly aeroelastic structures. Flutter suppression sensors would be a natural subcomponent of the aircraft's Structural Health Monitoring (SHM) system and could provide indispensable data for any Prognostics Health Management (PHM) system as well.

Vibration measurement systems can be used to monitor flutter and are also important for structural health monitoring because they can be used to detect structural damage and provide useful data in the localization and characterization of structural damage [5]. Traditionally, strain gauges [6, 7] and accelerometers [8] have been used to measure flutter on aircraft while more recent research has explored the use of microelectromechanical systems (MEMS) [9], PZT sensors [10-12], artificial hair from CNT [13], and fiber optic strain sensors [14, 15] in vibration and load monitoring applications. SAW devices are now being investigated for flutter applications because they are small, lightweight, low power, and can be deployed in a minimal-wiring daisy-chained layout. The potential for SAW devices to operate as a fully passive wireless device makes them particularly attractive.

In support of NASA's programs investigating high aspect ratio wings, a new method for measuring vibrations due to flutter has been developed based on Surface Acoustic Wave (SAW) sensors. Small, lightweight, low power flutter sensors are desirable for inclusion in new flexible aircraft structures and the retrofitting of existing aircraft that are exhibiting unwanted flutter phenomena. This new SAW-based flutter measurement technology has the potential to evolve into a wireless passive sensor platform that can detect flutter vibrations. Developing the wired sensor presented here is the first step towards the development of a wireless sensor network for flutter monitoring applications.

II. SENSOR DESCRIPTION

A SAW device vibration sensor was fabricated on Lithium Niobate ($LiNbO_3$) Y-Z cut substrate. The sensor has four orthogonal frequency coded (OFC) reflector banks, each with 3 MHz bandwidth, that combine to give a total reflection bandwidth of 12 MHz centered at 236 MHz (Fig. 1). The device is limited to two reflection tracks due to fabrication constraints. Each reflector bank is uniquely positioned in distance from the interdigitated transducer (IDT) to provide a unique position in time-of-flight for each reflector bank.

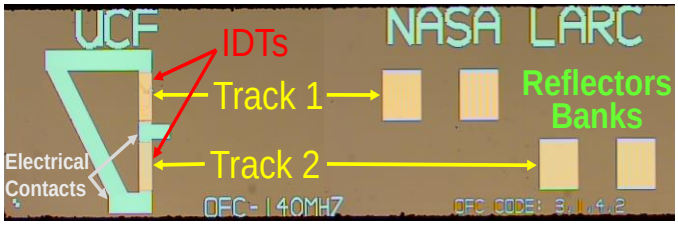

Figure 1. SAW OFC strain sensor. The tracks are shown in yellow and the IDTs, reflector banks, and electrical contacts are all identified in red.

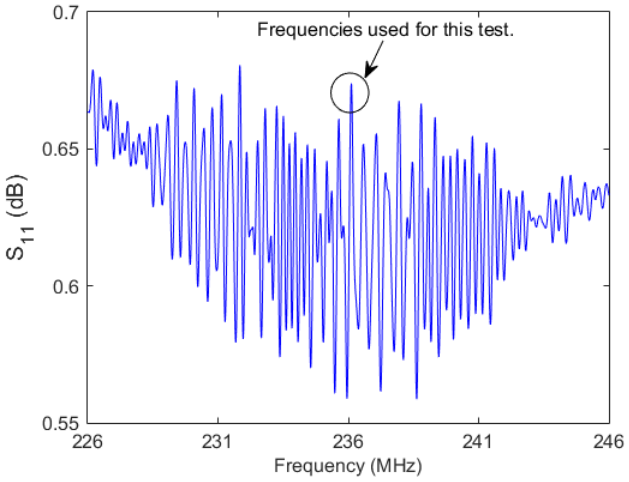

Figure 2. SAW S_{11} response The circle indicates the frequencies used for this work.

Simple strain and/or temperature measurements can be made by tracking the frequency response of the SAW device. Expansion, or lengthening, of a SAW device due to induced tensile strain or an increase in ambient temperature will result in a decrease in the operating frequency while contraction, or shortening, of the device will result in an increase in the operating frequency. The shift in operating frequency occurs because of physical changes which change the wavelength of the reflector banks and a change in the average propagation velocity of the surface acoustic wave, which is due to alterations in stiffness parameters and material density (acoustoelastic effects) [16]. This type of SAW device is interrogated by a chirp signal that is generated by a network analyzer. The S_{11} (reflection coefficient) response to the chirp signal is recorded by the network analyzer as the SAW measurement. The SAW S_{11} response has many rounded peaks and troughs, any of which could be used for strain measurements (Fig. 2). The subset of frequencies (236.055 MHz to 236.155 MHz) was chosen because it contained a peak within a 100 kHz frequency window. Note that the smaller the bandwidth the higher the frequency resolution for the same number of network analyzer measurement points. Also, note that the system takes snapshots (windows) of data, which are 100 KHz wide, and each snapshot captures multiple cycles of vibration events.

Shown in Fig. 3 is the sensing module utilized in this investigation. The aluminum enclosure contained two SAW devices; one device was bonded rigidly to the bottom of the package and the other device was bonded with a flexible bonding agent (RTV) in a layered fashion on top of a small layer of rubber with another layer of RTV in order to isolate it from strain effects. In past research efforts, this sensing module was used to measure strain in the rigidly-mounted device and temperature in the flexible mounted device to form a temperature compensated strain measurement [17]. In the effort presented here, vibration was measured using only the rigidly mounted device, as the particular processing used to measure vibration effects is negligibly affected by temperature changes.

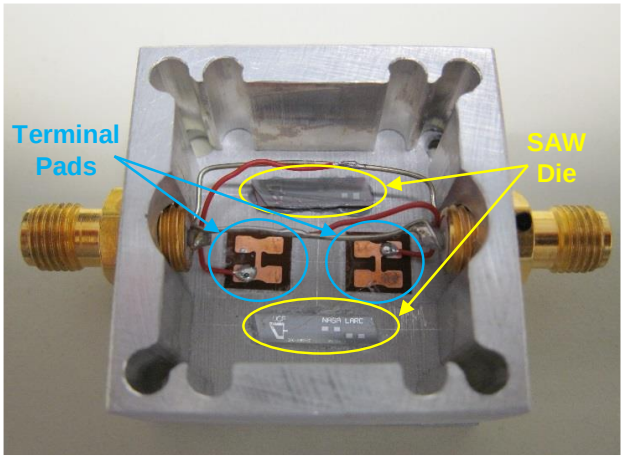

Figure 3. SAW sensor package, showing two SAW dies bonded inside, and two SMA connections. The terminal pads connect the SAW die to the SMA connectors. The bond wires that connect the die to the terminal pads are too small to be seen.

The module is designed so that multiple sensing modules can be daisy chained together through serially connected coaxial cable, yielding a multi-sensor, single channel configuration. Note that the devices use RF energy for both power and signals and therefore separate power cables are not required for operation. A long-term goal in the development of the SAW sensor technology is wireless interrogation; however, in near-term applications development the use of a single cable to connect multiple devices to a single interrogator gives the advantage of reduced wiring.

III. SAW Sensor Theory

The total frequency response FR_T is comprised of the sum of frequency response (or frequency shifts) due to environmental effects FR_E, and those due to flutter effects FR_F.

$$FR_T = FR_E + FR_F . \quad (1)$$

The frequency response is often used for flutter investigations [18]; however, for this work the relative phase shifts associated with the frequency shifts provide a better result.

The interrogation data from modern vector network analyzers can be delivered in a variety of formats: logarithmic magnitude, linear magnitude, phase, real, imaginary, or impedance. While the most common data format for SAW response analysis is the logarithmic magnitude response versus frequency, the influence of vibration effects on the magnitude-frequency response reduces to zero where the first derivative goes to zero at response maximums and minimums. That situation causes difficulty in the separation of combined environmental and vibrational effects represented in Eq. 1. However, collecting the relative phase of the response from the interrogator gives a separable vibrational response in the regions where the phase shifts are linear vs. frequency. In Fig. 4 a raw phase signal with a 2 Hz vibrational component (blue line) is plotted along with the low pass filtered phase signal (red dashed line) for a narrow band of frequencies (236.055 MHz to 236.155 MHz).

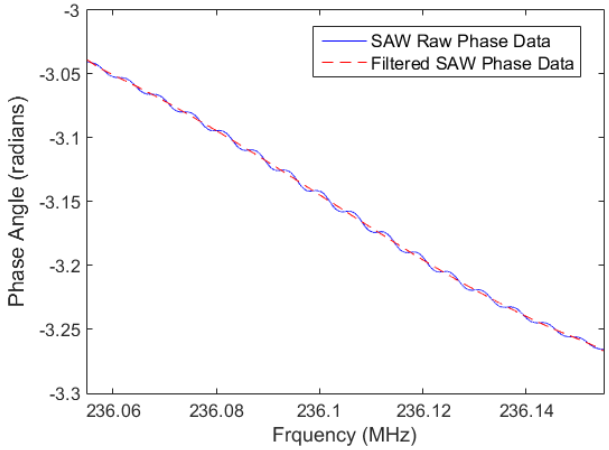

Figure 4. SAW raw phase data measuring a 2 Hz sine wave.

The phase decreases across the frequency range in a relatively linear manner. Filtering out the basic linear behavior of the phase response leaves a vibrational component that can be used for flutter measurements. Environmental effects are considered to be steady state, or extremely low frequencies below 1 Hz, and flutter vibrations are considered to be in the range of 1 Hz to 50 Hz for this investigation.

Subtracting the filtered SAW data from the raw SAW phase data results in the delta-phase data of Fig. 5.

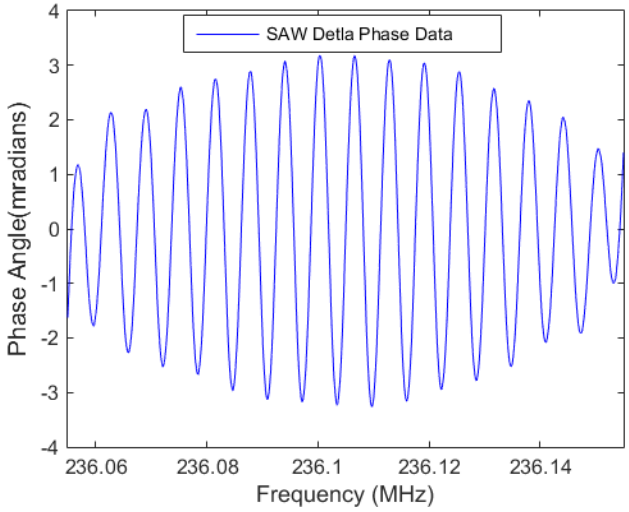

Figure 5. SAW delta-phase data resulting from subtraction of filtered phase data (Fig. 4 in red) from the raw phase data (Fig. 4 in blue).

The delta-phase data clearly shows the vibrational component, which matches the frequency of the panel vibration. However, the amplitude of the vibrational component rolls off at both ends of the frequency range. To correct for this phenomena, the data can be divided by the envelope of the data. The envelope, or analytic signal, can be generated by using the Hilbert transform. The Hilbert transform is calculated by using Eq. 2.

$$H[g(t)] = \frac{1}{\pi}\int_{-\infty}^{\infty}\frac{g(\tau)}{t-\tau}d\tau \,. \qquad (2)$$

The absolute value of the Hilbert transform of the delta-phase data is given in Fig. 6.

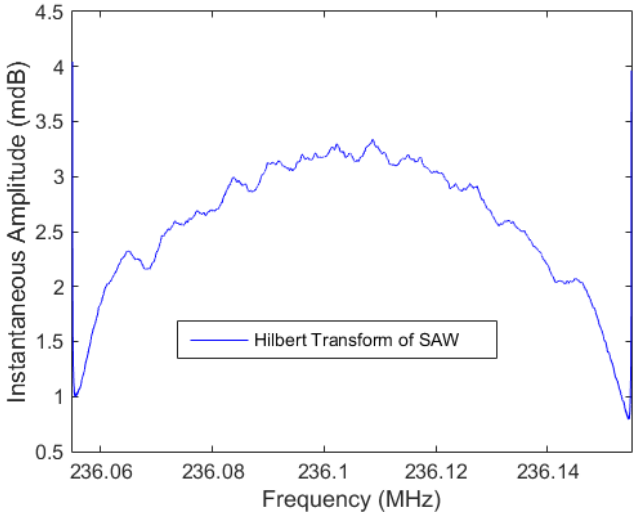

Figure 6. Hilbert transform of the filtered SAW delta-phase data.

The SAW vibration data shown in Fig. 7 is calculated by dividing the delta-phase data by the analytic signal, or Hilbert transform, of the delta-phase data

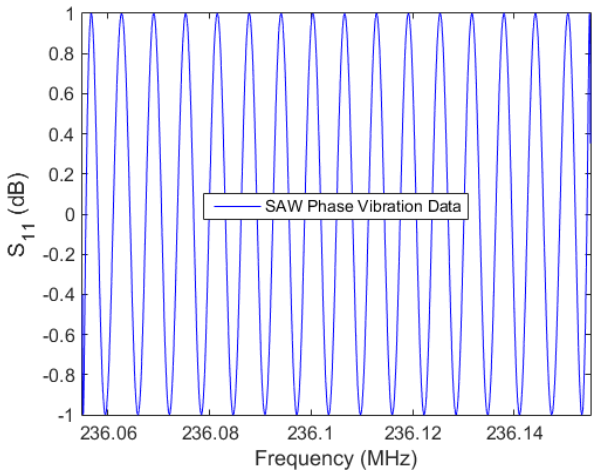

Figure 7. SAW vibration data, calculated by dividing the delta-phase data of Fig. 5 by the analytic signal of the delta-phase data of Fig. 6.

Passing the data through a low pass filter to remove high frequency noise and then using the Hilbert transform to detect the envelop yields a measurement that has a consistent amplitude for sinusoidal vibration signals (Fig. 7). It should be noted that this method only works to remove the distortions from signals that are cyclic in nature (flutter response) and is inappropriate for processing arbitrary broadband signals.

IV. Experimental Setup

For this work, a Carbon fiber–reinforced polymer (CFRP) composite panel measuring 406 mm by 406 mm by 2.78 mm was fabricated at NASA Langley Research Center. The composite laminate IM7/8552 is quasi-isotropic and is made up of IM7 fibers and 8552 prepreg material with a 26 ply thick layup of $[(0/+45/-45/90)_3\ 0]_S$. Details of the material properties are available in a prior paper by Leckey et al [19].

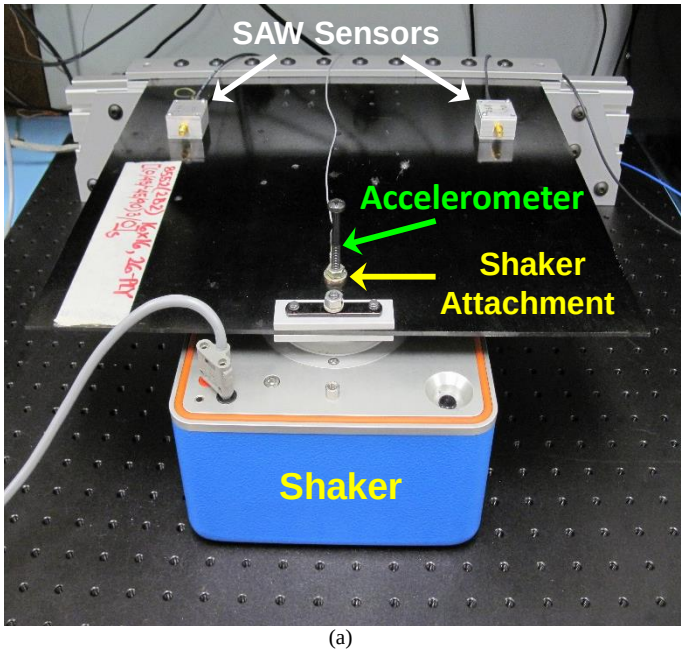

(a)

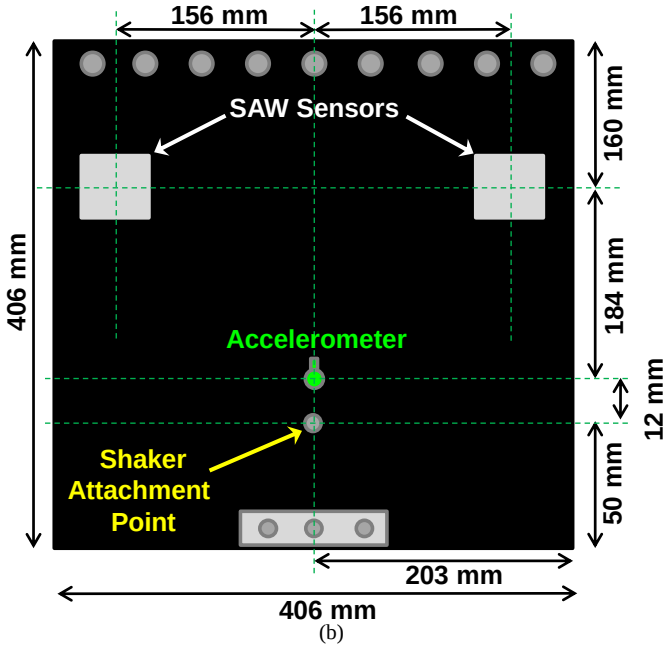

(b)

Figure 8. (a) Composite test panel. The SAW and accelerometer are mounted on top of the panel. The shaker is located at the free end of the cantilever underneath the panel. (b) A diagram showing the location and distances of the sensors and the shaker attachment location.

Both a SAW strain sensing module with a center frequency of 236 MHz and a Dytran Instruments, Inc. Miniature Accelerometer, model number 3035B1G, are bonded to the panel (Fig.8 (a)). The locations of the sensors are given in Fig. 8 (b). Only one of the two SAW sensing modules was utilized in this investigation.

An HP 8116A function generator was used to drive an APS Dynamics model 300-C Portable Shaker-Amplifier attached to the free end of the cantilevered panel to simulate flutter by inducing structural vibration. The SAW sensor was connected to an Agilent Technologies 6 GHz Network Analyzer, model N5230C, while the accelerometer signal was sampled using the National Instruments™ cDaq-9178 data acquisition system with a NI 9232 input module. The instrumentation operational schematic is shown in Fig. 9.

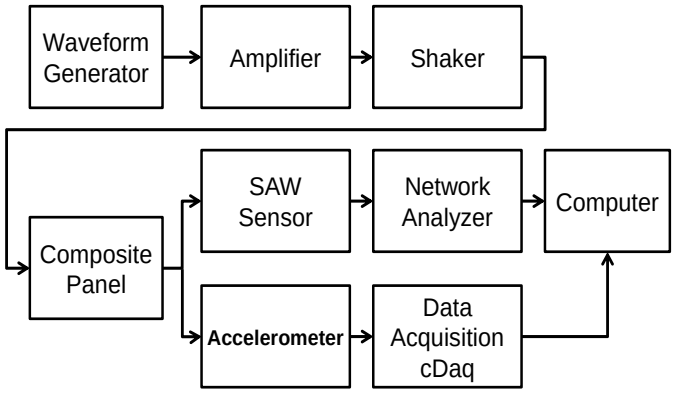

Figure 9. Instrumentation Diagram.

V. Results

To demonstrate the ability of the SAW sensor to detect flutter vibrations the SAW phase data was sampled and processed at the vibrational frequencies of 1 H, 2 Hz, 5 Hz, 10 Hz, 25 Hz, and 50 Hz using a sinusoidal driver signal 900m $V_{pk\text{-}pk}$ from the function generator. The SAW data of Figs. 10-15 have been normalized to the accelerometer data for the purpose of qualitative comparison. The results compare favorably with those from Bartels et al [20]. For the lower frequency cases (1H, 2Hz, and 5 Hz), the SAW sensor measurements show sinusoidal dynamics in the panel while the accelerometer data appears distorted. The source of the distortion in the accelerometer measurement is not certain, but is most likely related to the impulse response of the cantilevered panel and the shaker apparatus imparting distorted dynamics that do not appear in the SAW measurement due to the low-pass filtering/Hilbert transform normalization operation detailed previously. For the other three cases (10 Hz, 25 Hz, and 50 Hz), both the SAW sensor and accelerometer data show sinusoidal behavior and match each other closely.

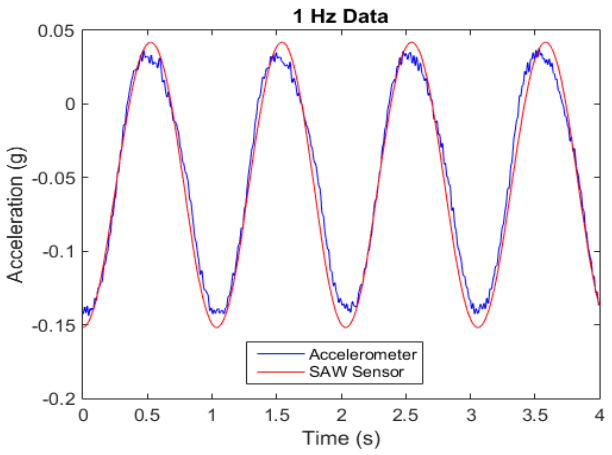

Figure 10. SAW and accelerometer data with a 1 Hz signal.

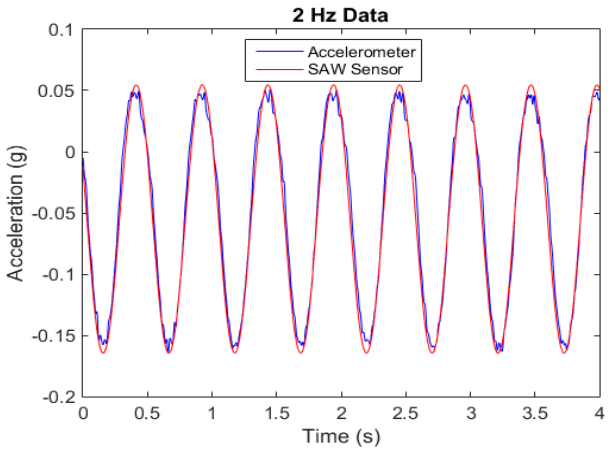

Figure 11. SAW and accelerometer data with a 2 Hz signal.

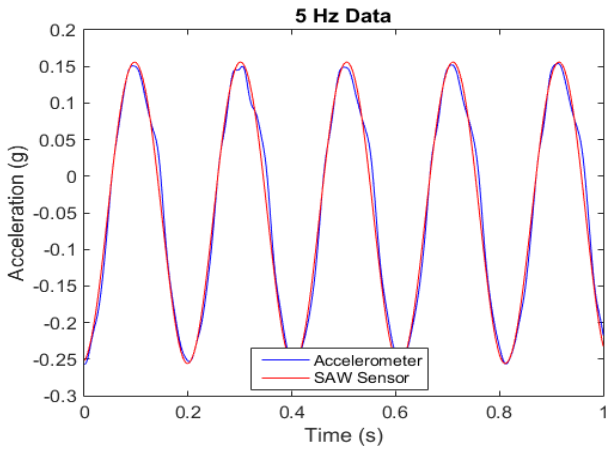

Figure 12. SAW and accelerometer data with a 5 Hz signal.

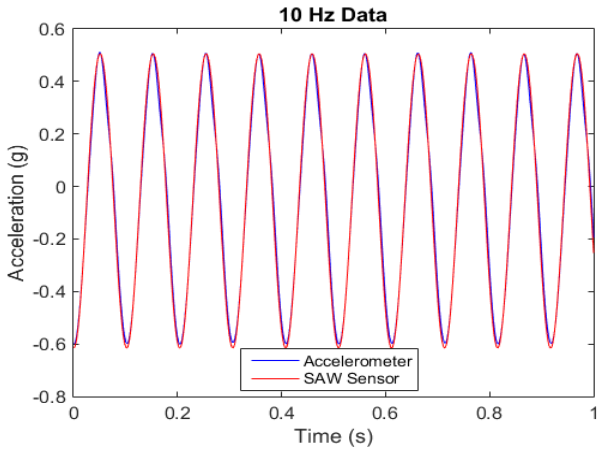

Figure 13. SAW and accelerometer data with a 10 Hz signal.

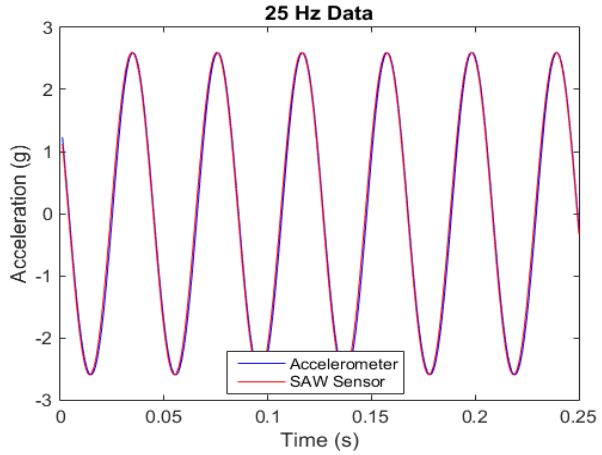

Figure 14. SAW and accelerometer data with a 25 Hz signal.

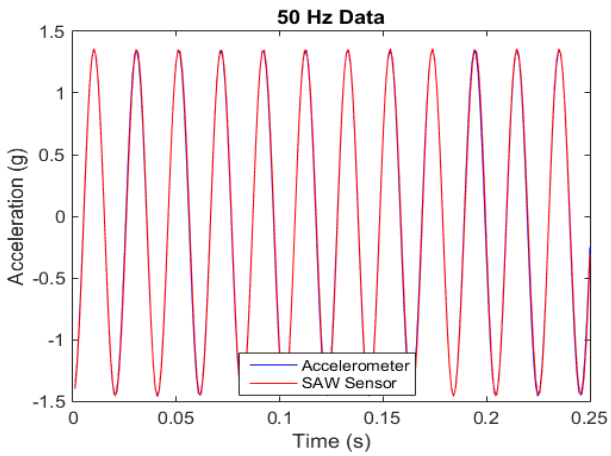

Figure 15. SAW and accelerometer data with a 50 Hz signal.

VI. Conclusions

A new method of employing low power SAW sensors to detect aeroelastic flutter phenomena has been presented. The SAW sensor data was compared to accelerometer data taken from a cantilevered panel vibrating at 1Hz, 2Hz, 5 Hz, 10 Hz, 25 Hz, and 50 Hz. For all six cases, the processed SAW sensor phase data yielded a vibrational behavior that qualitatively closely matches the accelerometer-measured vibrational input.

Further characterization of the device is needed. Testing the sensor while increasing and decreasing frequency of vibrations has been proposed. Future work includes designing a sensing module that will impart g-forces into the SAW device independent of structural surface strain to ultimately form a "place anywhere" passive wireless flutter detector. Higher TRL development and relevant environment testing in wind tunnels and flight tests are anticipated.

Acknowledgments

The authors would like to acknowledge Dr. Dan Gallagher and Dr. Donald Malocha at the University of Central Florida for help with design of the SAW devices and fabrication of the sensors.

References

[1] R. C. Scott, T. J. Allen, *et al.*, "Aeroservoelastic Wind-Tunnel Test of the SUGAR Truss Braced Wing Wind-Tunnel Model," presented at the 56th AIAA/ASCE/AHS/ASC Structures, Structural Dynamics, and Materials Conference, Kissimmee, Florida, AIAA 2015-1172, Jan. 5-9, 2015, p. 28.

[2] R. E. Bartels, R. C. Scott, *et al.*, "Aeroelastic Analysis of SUGAR Truss-Braced Wing Wind-Tunnel Model Using FUN3D and a Nonlinear Structural Model," in *Proc. 56th AIAA/ASCE/AHS/ASC Structures, Structural Dynamics, and Materials Conference*, Kissimmee, Florida, AIAA 2015-1174, Jan. 5-9, 2015, p. 15.

[3] J. J. Ryan, J. T. Bosworth, *et al.*, "Current and Future Research in Active Control of Lightweight, Flexible Structures Using the X-56 Aircraft," in *Proc. 52nd Aerospace Sciences Meeting*, National Harbor, MD, Jan. 13-17, 2014, pp. 1-11.

[4] J. R. Chambers, *Innovation in Flight: Research of the NASA Langley Research Center on Revolutionary Advanced Concepts for Aeronautics*: NASA History Division, NASA SP-2005-4539, 2005.

[5] D. Goyal and B. Pabla, "The Vibration Monitoring Methods and Signal Processing Techniques for Structural Health Monitoring: A Review," *Archives of Computational Methods in Eng.*, pp. 1-10, March 10 2015.

[6] M. J. Klepl, "A Flutter Suppression System Using Strain Gages Applied to Active Flexible Wing Technology: Design and Test," in *Proc. AIAA Dynamics Specialist Conference*, Dallas, TX, April 16-17, 1992, pp. 162-171.

[7] H. Teimouri, "A New Statistical Approach to Strain-Based Structural Health Monitoring of Composites Under Uncertainty," PhD, Mechanical Engineering, University of British Columbia, 2015, pp. 1-188.

[8] R. Samikkannu and A. Upadhya, "Wind Tunnel Flutter Testing of Composite T-Tail Model of a Transport Aircraft with Fuselage Flexibility," in *Wind Tunnels and Experimental Fluid Dynamics Research*, P. J. C. Lerner, Ed., INTECH Open Access Publisher, 2011, pp. 75-89.

[9] M. Martinez, B. Rocha, *et al.*, "Load Monitoring of Aerospace Structures using Micro-Electro-Mechanical Systems (MEMS)," in *Proc. ASME 2012 Conference on Smart Materials, Adaptive Structures and Intelligent Systems*, Stone Mountain, GA, September 19-21, 2012, pp. 799-805.

[10] C. Sathyanarayana, S. Raja, *et al.*, "Procedure to Use PZT Sensors in Vibration and Load Measurements," *Smart Materials Research*, vol. 2013, Article ID 173605, pp. 1-9, 2013.

[11] Z.-G. Song and F.-M. Li, "Active aeroelastic flutter analysis and vibration control of supersonic beams using the piezoelectric actuator/sensor pairs," *Smart Materials and Structures*, vol. 20, no. *5*, *055013*, pp. 1-13, 2011.

[12] F. Nitzsche, D. D'Assunção, *et al.*, "Aeroelastic Control of Non-Rotating and Rotating Wings using the Dynamic Stiffness Modulation Principle Via Piezoelectric Actuators," *Journal of Intelligent Material Systems and Structures*, pp. 1-13, 2015.

[13] W. Su and G. W. Reich, "Gust Alleviation of Highly Flexible UAVs with Artificial Hair Sensors," in *Proc. SPIE Smart Structures and Materials & Nondestructive Evaluation and Health Monitoring*, 2015, pp. 94350X 1-14.

[14] S. Cinquemani, G. Cazzulani, *et al.*, "Vibration Control of Shell-Like Structures with Optical Strain Sensors," in *Proc. Active and Passive Smart Structures and Integrated Systems*, San Diego, CA, March 10-13, 2014, pp. 90572Z 1-7.

[15] H. V. Thakur, S. M. Nalawade, *et al.*, "All-Fiber Embedded PM-PCF Vibration Sensor for Structural Health Monitoring of Composite," *Sensors and Actuators A: Physical*, vol. 167, no. *2*, pp. 204-212, 2011.

[16] K.-y. Hashimoto, *Surface acoustic wave devices in telecommunications: modelling and simulation*. Berlin: Springer Verlag, 2000.

[17] W. C. Wilson, M. D. Rogge, *et al.*, "Fastener Failure Detection Using a Surface Acoustic Wave Strain Sensor," *Sensors Journal, IEEE*, vol. 12, no. *6*, pp. 1993-2000, June 2012.

[18] T. Wei, S. Zhongke, *et al.*, "Aircraft Flutter Modal Parameter Identification Using a Numerically Robust Least-Squares Estimator in Frequency Domain," *Chinese Journal of Aeronautics*, vol. 21, no. *6*, pp. 550-558, 2008.

[19] C. A. Leckey, M. D. Rogge, *et al.*, "Guided Waves in Anisotropic and Quasi-Isotropic Aerospace Composites: Three-Dimensional Simulation and Experiment," *Ultrasonics*, vol. 54, no. *1*, pp. 385-394, 2014.

[20] R. E. Bartels, R. C. Scott, *et al.*, "Computed and Experimental Flutter/LCO Onset for the Boeing Truss-Braced Wing Wind-Tunnel Model," in *Proc. 44th AIAA Fluid Dynamics Conference*, Atlanta, GA, AIAA 2014-2446, June 16-20, 2014, p. 24.